EIS study to analyse the influence of mechanical compression on the global PEM fuel cell performance

El Mahdi Khetabi, Khadidja Bouziane, Xavier François, Remy Lachat, Yann Meyer, Denis Candusso

EIS study to analyse the influence of mechanical compression on the global PEM fuel cell performance

El Mahdi KHETABI[1], Khadidja BOUZIANE[1], Xavier FRANÇOIS[2], Remy LACHAT[3], Yann MEYER[4], Denis CANDUSSO[1]
[1] Université Gustave Eiffel, Université Paris Saclay, ENS Paris Saclay, SATIE, COSYS, FCLAB, 90010 Belfort Cedex, France.
[2] Université Bourgogne Franche-Comté, UTBM, FCLAB, 90010 Belfort Cedex, France.
[3] ICB, CNRS, Université Bourgogne Franche-Comté, UTBM, 90000 Belfort, France.
[4] Université Savoie Mont Blanc, SYMME, 74000 Annecy, France.

Abstract:
Proper clamping pressure is needed to guarantee the gas-tightness of PEMFC assembly and to enhance the contacts between components. Nevertheless, excessive mechanical load can deteriorate the cell performance, particularly by reducing the porosity and the mass transfer properties of the Gas Diffusion Layers (GDLs). In this study, the global performance of a 225 cm² PEMFC assembly under mechanical stress (0.35 - 2 MPa) is investigated through Electrochemical Impedance Spectroscopy (EIS) as a complement to cell voltage monitoring and polarisation curves carried out previously. The analysis relies on the evolution, against mechanical compression, of the high and low frequency resistances, as well as the arc sizes of the EIS spectra. The measurements emphasise that mechanical loading primarily decreases ohmic losses, and they also highlight the importance of harmful physical phenomena at high frequencies. Ex-situ measurements (through-plane resistance of GDL) and in-situ results (high frequency resistance) show a similar reduction trend observed with increasing mechanical compression.

Keywords: PEMFC; Clamping pressure; Mechanical assembly; EIS; Gas Diffusion Layer.

Highlights:
- The effect of clamping on the electrical behaviour of a 225 cm² PEMFC is studied.
- A mechanical compression unit is used to apply loads (0.35 - 2 MPa) on the cell.
- Effect of compression is investigated using Electrochemical Impedance Spectroscopy.
- Mechanical load reduces ohmic losses and harmful high frequency physical phenomena.
- The tests are correlated with ex-situ measures of GDL resistances.

1. Introduction

A Proton Exchange Membrane Fuel Cell (PEMFC) assembly is a multi-contact structure where various physical phenomena are intricately interlinked. The mechanical stress within the assembly stands out as a primary factor influencing both the electrical performance and durability of the Fuel Cell (FC) [1-7]. Currently, two primary characterisation approaches are utilised to examine the effects of clamping pressure on FC performance. The first is an ex-situ type approach, where individual elements are assessed outside the FC. The second is a set of in-situ methods, where the behaviours of the components are evaluated within an operating FC. Researchers employing these ex-situ and in-situ characterisation techniques in the study of PEMFCs are emphasising specific aspects, including (1) electro-physical properties of Gas Diffusion Layers (GDLs) [8-10], (2) identification of mass transfer limitations [11-13], (3) assessment of durability [14-17], (4) visualisation techniques for water transport [18-20], and (5) analysis of mechanical stress distribution in the GDL and cell [21-29]. Given the intricate nature of the phenomena involved, effective diagnosis of PEMFCs necessitates well-suited techniques capable of evaluating all the aforementioned issues and distinguishing their respective impacts on the overall FC performance. To date, beyond simply observing the FC voltage, researchers have commonly employed two established methods for studying the impacts of clamping pressure: polarisation curve (U-I) measurements [7] and, to a lesser extent, Electrochemical Impedance Spectroscopy (EIS) records [30-36].

The aim of our research work is to explore the influences of mechanical compression on PEMFC performance. The investigations involve two key aspects: i) utilising in-situ characterisations and ii) examining correlations with ex-situ results conducted within the MIREPOIx project, which encompasses both in- and ex-situ studies [7, 37-41].

In our previous publication within this project [42], the objective was to comprehensively elucidate how mechanical compression quantitatively influences the overall performance of the cell. This was achieved through a combination of steady-state measurements, i.e. FC voltage monitoring and U-I curve records. The resulting analysis provided guidelines for researchers and industry professionals, offering insights into the effects of mechanical compression and facilitating the optimisation of FC performance. Figure 1. illustrates examples of polarisation curves measured at various mechanical stress levels. The U-I plot incorporates two zoomed-in regions at medium and high current densities, along with the corresponding changes in stack voltage in relation to compression. The trend is noticeable: the cell voltage rises with increasing mechanical compression at all current ranges, particularly from 0.35 to 1.1 MPa [42].

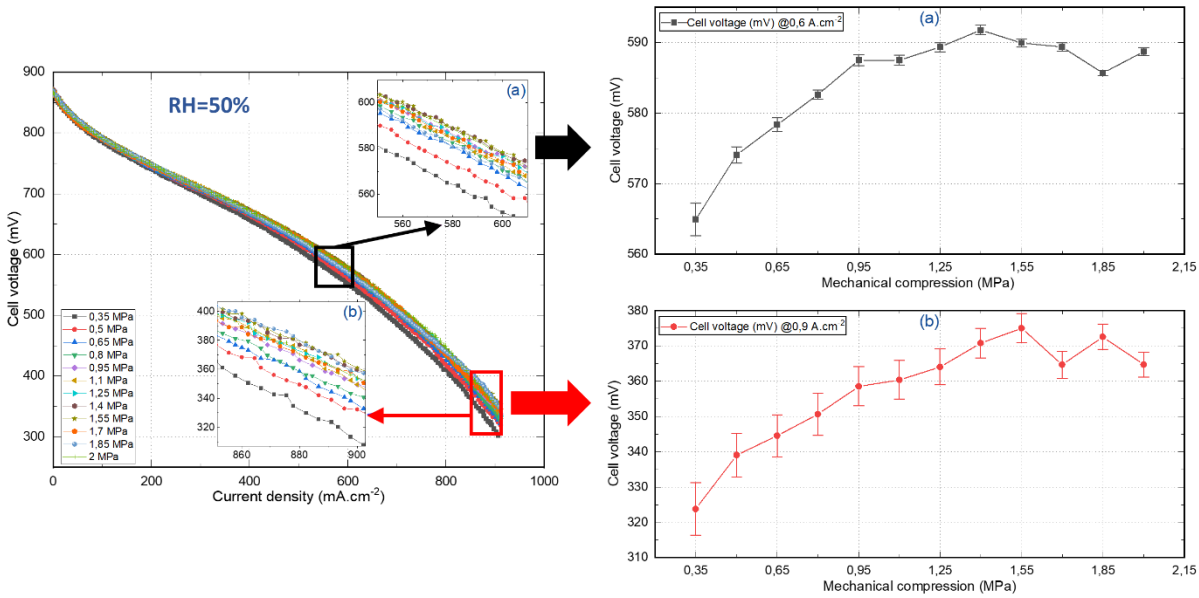

Fig. 1. Example of polarisation curves recorded for 12 levels of mechanical compression (left); inserts (a) and (b) are zoomed-in regions at medium and high current densities. The related voltage evolution as a function of mechanical compression: (a) at 0.6 A cm^{-2} and (b) at 0.9 A cm^{-2} (right).

In the present article, we intend to show how EIS records, used in complement to voltage monitoring and polarisation curves, can help to better distinguish between the different types of electrical phenomena involved in the cell under mechanical stress and thus improve our understanding of the phenomena studied.
The structure of this article is as follows. In Section 2, we provide a concise overview of the experimental set-up developed for our study, which includes details about the FC test bench, the dedicated mechanical compression unit, and the components of the investigated PEMFC. The procedures implemented in the experiments are outlined in Section 3. Moving on to Section 4, we analyse the EIS results and present quantitative findings regarding the effects of compressive stress on the phenomena taking place in the FC.

2. Experimental equipment and PEMFC components

A specially designed testing apparatus is devised to explore the impacts of mechanical compression on PEMFC performance. The setup enables both mechanical and electrical characterisations of a single PEM cell under various operational conditions and compression levels. This equipment comprises:

- A dedicated PEMFC test stand: designed for controlling the reactants, the cell temperature, and the electronic load [38, 42]. The bench (G7805 from Greenlight Innovation® [43]) can interface with an EIS station (Materials Mates [44]). Further information about this EIS station will be provided in Section 4.
- A specifically crafted Mechanical Compression Unit (MCU) (batlticFuelCells [45]): 4 pneumatic cylinders are used to exert controlled mechanical constraints (up to 2.15 MPa) on the assembly of a PEM single cell with an active area equal to 225 cm^2 [38, 42]. This large surface holds relevance to potential real-world applications. A picture of the MCU can be seen in the Graphical abstract.

- A compression regulation system and displacement measurement device: used for the regulation of the compression applied and the measurement of the displacement in thickness of the single cell as a function of the operating conditions.
- A device for measuring local currents and temperatures within the cell [38].

Details regarding the individual components of the investigated single cell are provided below and in [38, 42].
- Membrane Electrode Assembly (MEA): The 3-layer component incorporates Catalyst Layers (CLs) with platinum loadings of 0.2 mg $Pt.cm^{-2}$ at the anode and 0.4 mg $Pt.cm^{-2}$ at the cathode. The membrane utilised is a Nafion™ XL [46, 47].
- GDL: A Sigracet® 38 BC (SGL Carbon [48]) is selected. It is a non-woven carbon paper, coated with a MPL and PTFE-treated, and recognised as a low porosity GDL in comparison to other types (Sigracet® 39 BC for example), making it particularly suitable for use conditions below 50% Relative Humidity (RH) [49].
- Flow Field Plates (FFPs): Plates in graphite, grade FU 4369 HT (Schunk [50]), are used in the tests. These FFPs adopt a parallel serpentine design, featuring 12 parallel channels, with a land width and channel width of 0.96 and 1 mm, respectively.

3. Experimental procedures

In order to understand how the mechanical pressure quantitatively influences the PEMFC electrical behaviour, investigations are conducted using EIS while subjecting the cell to mechanical constraints. The FC operating conditions are described hereafter, as well as the parameters studied and the mechanical compression protocol used during the EIS characterisations. Additional details on the procedures applied for the preliminary tests (leak tests, break-in, conditioning) and the previous steady-state experiments can be found in [38, 42].
The FC temperature is kept constant at 60°C. The cell is operated with air and high-purity H_2 (5.0 quality) at constant cathode and anode flowrates, which have been determined as optimal for a 0.9 A cm^{-2} current density (air and H_2 flow rates set at 19.1 and 2.4 $Nl.min^{-1}$, respectively). The gases are introduced in a flow-through mode, maintaining anode and cathode back-pressures at 50 kPa and Relative Humidity rates at 50%RH. These operating conditions lead to the highest and most stable cell performance [38, 42]. They remain constant in the EIS tests, with our primary focus directed towards observing variations in current density and mechanical compression.
A total of twelve compression levels are implemented on the PEMFC, spanning from 0.35 to 2 MPa with incremental increases of 0.15 MPa (See Graphical abstract). The duration of each compression level, set at intervals of 300 seconds, is selected to ensure the settling of materials and the stabilisation of performance before transitioning from one pressure level to another. This compression protocol was also adopted for polarisation curve measurements (Fig. 1) [38, 42]. It allows us to study in detail the effect of increasing mechanical stress within the PEMFC. It can also mirror the gradual stresses that may arise inside the cell, such as those encountered during the PEMFC assembly process. The impact of compression is studied for two current densities, equal to 0.6 and 0.9 $A.cm^{-2}$, and corresponding to FC operating regions where ohmic and mass transfer phenomena carry significant importance. These current densities will be denoted as medium and high current density, respectively.

4. EIS records and analyses

4.1. Principles

Electrochemical Impedance Spectroscopy (EIS) is a characterisation technique widely used for PEMFC performance assessment [30,31,51,52]. The phenomena involved within the PEMFC and their dynamics can be to some extent dissociated by varying the frequency of a sinusoidal input current (in galvanostatic mode) and observing the induced voltage. The impedance $\overline{Z}(f)$ of the PEMFC can be represented, as a function of frequency f, in the Nyquist diagram, as shown by the illustration of Fig. 2. In this example, two arcs are discernible: High Frequency (HF) arc and Low Frequency (LF) arc, from left to right. They may be representative of charge transfer and mass transport phenomena, respectively. The combination of these two arcs illustrates the dynamic behaviour of a PEMFC in response to current excitation over a wide range of frequencies (some mHz to tens of kHz). In studies examining cell compression with EIS characterisation [30-36], the overlap between the HF and LF arcs varies, often making them challenging to distinguish with precision [30].

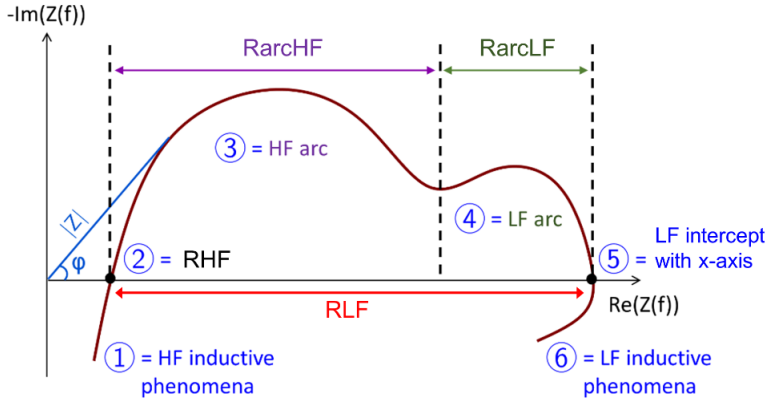

Fig. 2. Example of a PEMFC impedance spectrum $\overline{Z}(f)$ plotted in the Nyquist diagram, with the geometric characteristics used in the study.

The physical phenomena that take place within the PEMFC and that describe its dynamic behaviour occur at different timescales. Some phenomena have time constants of the order of a microsecond (e.g. ohmic resistance) whereas others have time constants on the scale of several minutes (e.g. phenomena of hydration and humidification of the membrane). Therefore, the shape of the impedance spectrum shown in Fig. 2., and its different regions with numbers coloured blue, can be explained by the following electrochemical processes taking place within the PEMFC:

1. The first information that appears on the spectrum starting from high frequencies (tens of kHz to some kHz) concerns inductive phenomena related to the wires and electrical connections of the test system (neither related to the PEMFC itself nor to its electrochemical phenomena). This HF inductive phenomenon is represented by a crossing of the impedance spectrum towards the positive imaginary axis [53].
2. The High Frequency Resistance (RHF) is representative of the ohmic resistance of the PEMFC, which is composed of the protonic resistance of the membrane [32] and the bulk electronic resistance of the cell components along with their respective electrical contact resistances [54]. The ohmic resistance is determined by the intersection between the impedance spectrum and the real axis at high frequencies range (typically between 1 and 10 kHz). The higher mechanical pressure reduces contact resistances, and thus RHF [30-36]. Some works show that clamping has a predominant impact on RHF [34].

3. The High Frequency arc is partly representative of charge transfer phenomena and thus represents the transfer and accumulation of electric charges at the electrode-electrolyte interfaces. The magnitude of this HF arc (as depicted by the RarcHF parameter in Fig. 2) is prominent at lower current densities, gradually diminishing in size as current levels increase, in proportion to the LF arc. The effect of mechanical compression on the size of the HF arc seems to be little discussed in the literature. According to Dotelli et al. [31], increasing mechanical compression enhances contacts between GDL and CL, thereby promoting electron transfer processes and resulting in a decrease of RarcHF in Fig. 2.
4. The Low Frequency arc is commonly associated with mass transport phenomena (i.e. diffusion of species) from the channels to the catalyst layer. The dimensions of this arc (as represented by the RarcLF parameter in Fig. 2) notably expand under high current densities, due to hindered diffusion of reactants within the cell. Depending on the range examined, heightened mechanical compression may lead to a reduction in pore size within the GDL beneath the rib of the flow field plate, thus impeding gas diffusion and increasing RarcLF [33].
5. The low-frequency Resistance (RLF) can be referred to as polarisation resistance (regardless of RHF). In this study, the RLF value is the distance on the Nyquist plot between the two intercepts with the x-axis (i.e. the distance between RHF and the intercept at low frequencies ranging from 10 to 100 mHz) (Fig. 2).
6. The last region of the spectrum, at low frequencies range, corresponds to the pseudo-inductive loop, which is still a subject of research in the literature. In the review study of Pivac and Barbir [53], two major interpretations have been identified as plausible: water transport characteristics and side reactions with intermediate species. This latter along with the HF inductive phenomenon will not be addressed in this article.

The electrochemical processes described in this section can be modelled using equivalent electric circuits models. However, in this article, taking a practical approach, we will mainly consider the values of the High and Low Frequency resistances (RHF and RLF) of the EIS spectra to analyse the effects of the compression on the PEMFC dynamical performance. The respective sizes of the High and Low Frequency arcs will also be considered in our analysis through the RarcHF and RarcLF parameters (used actually as geometric descriptors of the EIS spectra, the RLF resistance being represented by the width of the two arcs with RLF = RarcHF + RarcLF) (Fig. 2).

Our study aims to investigate separately, as far as possible, the impacts of mechanical compression on the ohmic resistance, as well as on the High and Low Frequency phenomena. The analysis of the effects of mechanical stress on the PEMFC electrical response will be based on the investigations of the evolution of the RHF, RLF, RarcHF, RarcLF resistances, measured directly from the experimental impedance spectra.

Note that the low-frequency intercept with the real axis was not consistently attained during our EIS experimentations. Therefore, the RLF was measured from the corresponding $\mathrm{Re}\left(\overline{Z}(f)\right)$ obtained at the nearest point to the real axis.

4.2. EIS results and discussion

The EIS station used in our tests (Materials Mates, Italy [44]) includes different modules: a power unit of 1.5 kW (0-50V) reversible in current (±50A), a single-channel master frequency analyser for the FC stack voltage, and a 12-channel frequency analyser for the single cell voltages of the FC. The current perturbation signal is set at 8% of the DC current delivered by the PEMFC and is applied from 1 kHz to 100 mHz at 10 points per decade.

4.2.1. Effect of current density on RHF and RLF

Figure 3. shows the impedance spectra at different levels of mechanical compression. As in the previous experimental procedures (i.e. steady-state characterisation techniques [42]; Fig. 1), EIS analyses are conducted at current densities of 0.6 and 0.9 A.cm^{-2}. For clarity purposes, only three levels of mechanical compression are depicted per each current density level. The goal of this subsection is to study the effect of current density on the contribution of the resistances RHF and RLF. The estimation of the different phenomena taking place within the PEMFC, according to mechanical stress, is detailed in the following subsections.

Regarding RHF: The results of the RHF evolution obtained from Fig. 3. are given in Table 1. The ohmic resistance is noticeably lower at 0.9 A.cm^{-2} in comparison to 0.6 A.cm^{-2}. This difference was measured to be 4% and was attributed to the increased presence of water on the cathode side for a current density of 0.9 A.cm^{-2}, which favours the back-diffusion water transport mechanism as we have previously illustrated in [42]. This effect, in turn, enhances the membrane humidification and leads to a lower ohmic resistance at 0.9 A.cm^{-2} compared to 0.6 A.cm^{-2}. These results, therefore, confirm the explanations given in [42] using the polarisation curves and PEMFC voltage monitoring techniques.

Regarding RLF: The RLF increases with higher current density as it can be seen from Fig. 3. This effect can be ascribed to the rise in the mass transport resistance due to the elevated water production rate at 0.9 A.cm^{-2}. Table 1. presents the contribution of the RarcHF and RarcLF resistances in the RLF. At medium current density (i.e. 0.6 A.cm^{-2}), the RarcHF contributes significantly in the RLF (67% on average) compared to the RarcLF, which can be attributed to the dominance of the activation resistance at this current density level. However, at high current density (i.e. 0.9 A.cm^{-2}), the RarcLF contribution in the RLF becomes substantially high (65% on average). This latter effect stems from the increased rate of liquid water production at the cathode side at 0.9 A.cm^{-2} compared to 0.6 A.cm^{-2}. By comparing the results shown in Table 1. at high and medium current densities, it can be observed that the RarcLF is about 4.7 times higher at 0.9 A.cm^{-2} compared to 0.6 A.cm^{-2}, whereas the RarcHF is about only 1.2 times higher at 0.9 A.cm^{-2} compared to 0.6 A.cm^{-2}. These results confirm the dominance of the mass transfer phenomena at high current density due to the higher water production rate at the cathode CL.

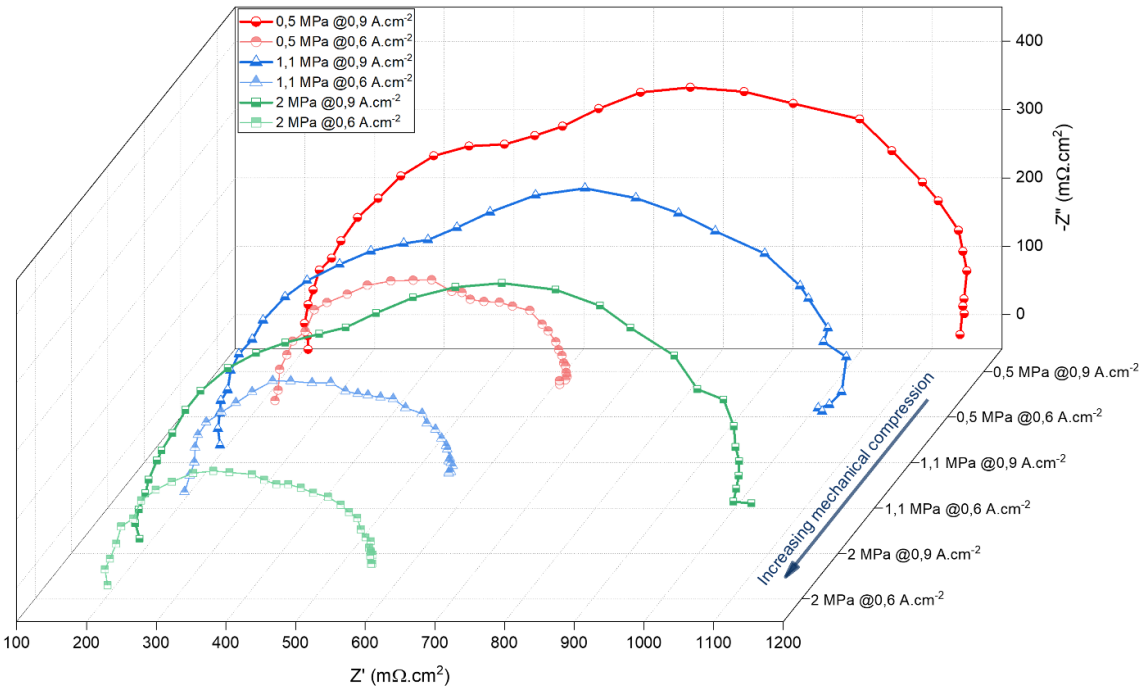

Fig. 3. Impedance spectra for three levels of mechanical compression at 0.6 and 0.9 A.cm^{-2}.

	Compression of 0.5 MPa (mΩ.cm^2)			Compression of 1.1 MPa (mΩ.cm^2)			Compression of 2 MPa (mΩ.cm^2)		
	RHF	RLF		RHF	RLF		RHF	RLF	
		RarcHF	RarcLF		RarcHF	RarcLF		RarcHF	RarcLF
Current density of 0.6 A.cm^{-2}	239.8	295.2 (73%)	108.4 (27%)	217.7	241.3 (65%)	130.5 (35%)	200.7	246 (64%)	135.4 (36%)
Current density of 0.9 A.cm^{-2}	230.2	326 (35%)	610 (65%)	205.6	301.7 (35%)	565.4 (65%)	191.5	302.1 (34%)	582.3 (66%)

Table 1. The evolution of the RHF resistance, the contribution of RarcHF and RarcLF resistances in the RLF resistance as a function of the current density at three levels of mechanical compression.

4.2.2. Effect of mechanical compression

- At medium current density: Figure 4. depicts the impedance spectra of 12 levels of mechanical compression at 0.6 A.cm^{-2}. It can be observed from insert (a) that the mechanical pressure reduces the ohmic resistance of the PEMFC, which is in good agreement with the first explanations given in [42] using steady-state characterisation techniques. However, insert (b) shows that mechanical compression also reduces the RLF. This effect, which was not typically reported in the literature [5-7], could be attributed to the decrease in the charge transfer resistance, as will be discussed further.

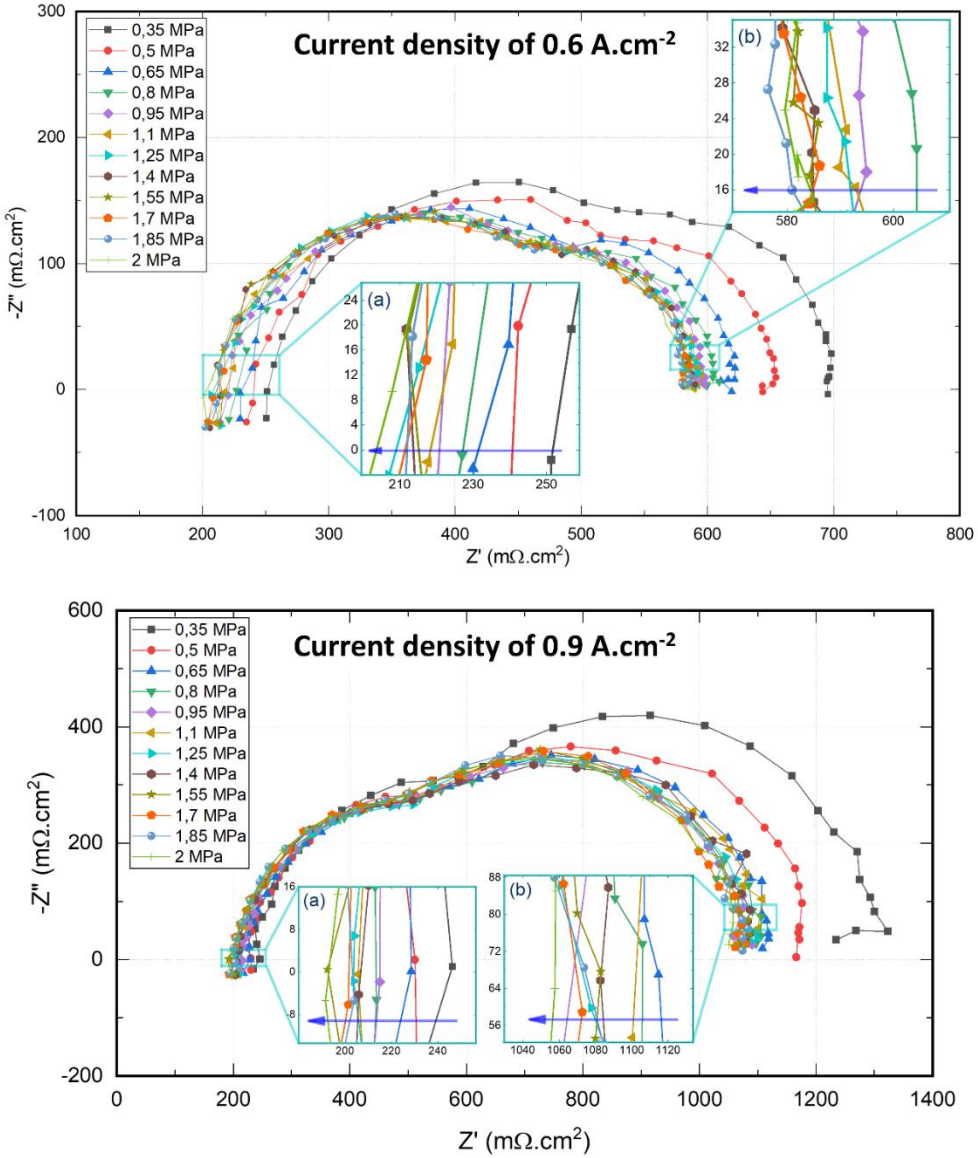

Fig. 4. Impedance spectra of 12 levels of mechanical compression at current densities of 0.6 A.cm^{-2} (top) and 0.9 A.cm^{-2} (down). Inserts (a) and (b) represent the RHF and RLF regions, respectively. The horizontal arrows represent the increase in the mechanical compression.

Regarding RHF: Figure 5. a). shows the evolution of the RHF according to mechanical compression at a current density of 0.6 A.cm^{-2}. It can be noticed that the ohmic resistance declines with increasing mechanical load, with an 18.3% decrease attained at 1.4 MPa over a total decrease of 20.1% reached at 2 MPa. This ohmic resistance diminution is attributed to the reduction in the electrical contacts and bulk resistances with increasing mechanical compression. In line with these results, K. Bouziane conducted, in the MIREPOIx research project, several ex-situ measurements on the effect of mechanical stress on the through-plane resistance of the same GDL investigated in this in-situ study (i.e. Sigracet® 38 BC) [39]. The ex-situ results are reported in Fig. 6. The through-plane resistance evolution depicted in this figure shows a nonlinear reduction tendency with mechanical compression. This reduction in the through-plane resistance is explained by the improved electrical connections of the carbon fibres with increasing mechanical compression. Results depicted in Fig. 6. show that 77.8% diminution of the through-plane resistance was attained starting from 0.5 MPa. The decrease at 1.5 MPa was measured to be 88.6% over a total decrease of 91.6% at 2 MPa. These findings corroborate the outcomes of the in-situ investigations shown in Fig. 5. a).

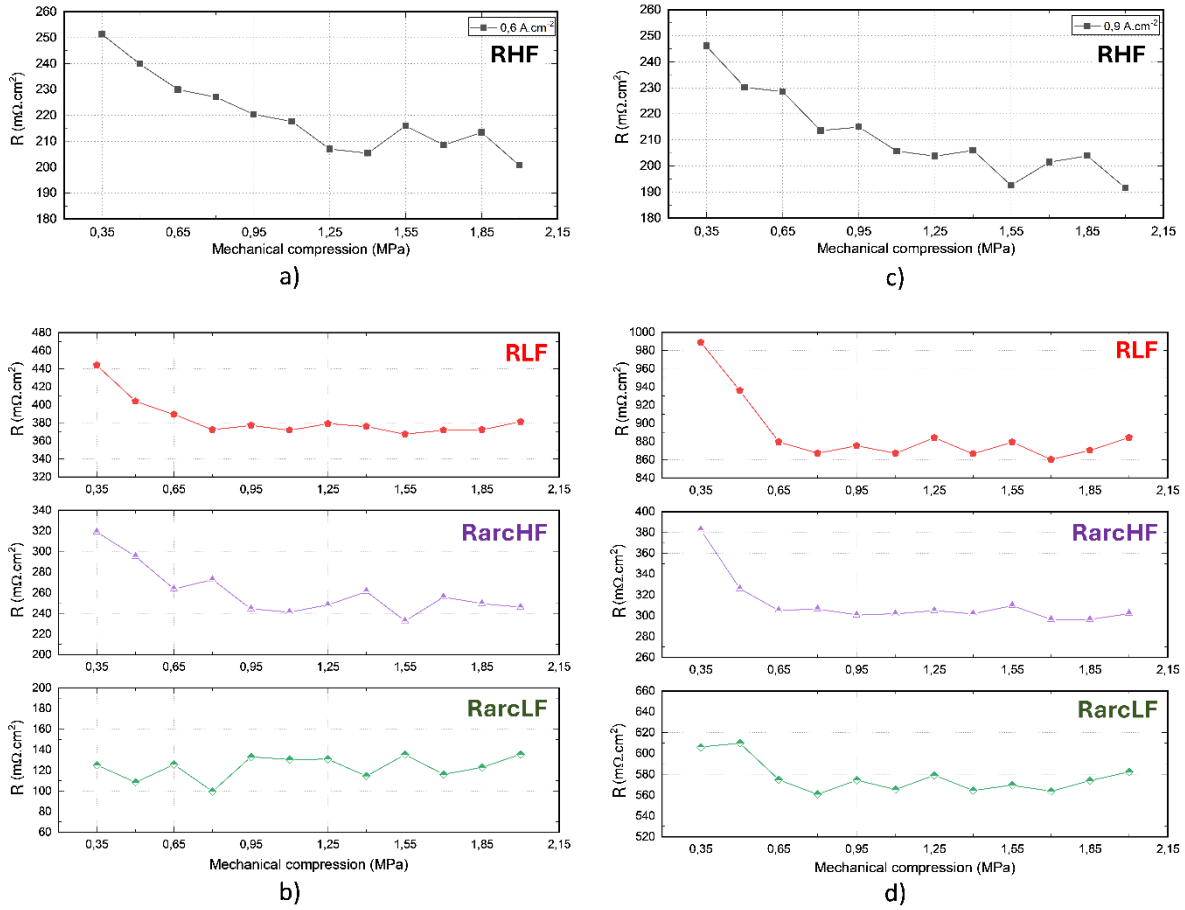

Fig. 5. The evolution of RHF, RLF, RarcHF, and RarcLF (with RLF = RarcHF + RarcLF) vs. mechanical compression at 0.6 A.cm^{-2} (left) and 0.9 A.cm^{-2} (right).

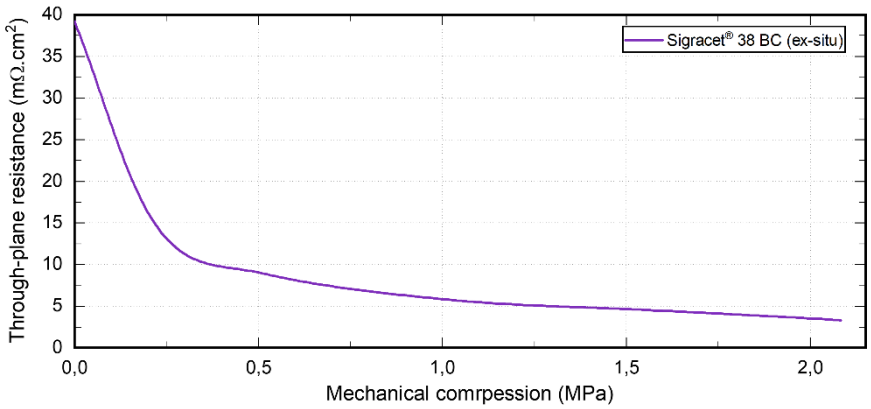

Fig. 6. Evolution of GDL through-plane resistance vs. mechanical compression - ex-situ measurements at 50°C [39].

Regarding RLF: Figure 5. b) shows the evolution of the RLF along with the contributions of RarcHF and RarcLF as a function of mechanical constraint at 0.6 A.cm^{-2}. The trend reveals a reduction in RLF as mechanical pressure increases, with a sharp decline of 16% at 0.8 MPa over a maximum decrease of 17% at 1.55 MPa. This RLF decrease during the initial compression range (0.35 - 0.80 MPa) is due to the diminution of RarcHF, which experienced a 27% reduction. Concurrently, RarcLF increased by 8% within the same compression range. It can be deduced from Fig. 5. b) that the decline in RLF with increasing mechanical pressure

is mainly due to the decrease in RarcHF, while RarcLF evolution represents a barely increasing tendency.

- At high current density: Figure 4. (down) shows the impedance spectra of 12 levels of mechanical compression at 0.9 A.cm^{-2}. Similar to the results reported at medium current density, it can be observed that mechanical stress reduces both the RHF and the RLF resistances at 0.9 A.cm^{-2}.

Regarding RHF: The RHF evolution as a function of mechanical compression at 0.9 A.cm^{-2} is depicted in Fig. 5. c). Consistently with the results reported at 0.6 A.cm^{-2}, the RHF resistance at 0.9 A.cm^{-2} decreases at higher mechanical pressures, with a 21.8% decrease attained at 1.55 MPa, over a 22.2% decrease at 2 MPa. These findings are attributed to the reduction in the ohmic resistance of the FC components. The RHF measured at 0.9 A.cm^{-2} is 4%, on average, lower compared to the RHF obtained at 0.6 A.cm^{-2}. This difference is ascribed to the better PEM hydration at elevated current density stemming from a higher water production rate at the cathode CL, and resulting in a significant back-diffusion transport mechanism for water. These results confirm the explanations given previously in [42] using steady-state techniques.
Regarding RLF: The evolution of the RLF is shown in Fig. 5. d). along with the contributions of RarcHF and RarcLF as a function of mechanical compression for 0.9 A.cm^{-2}. An observable trend is the decrease in RLF with an increase in mechanical pressure, which is mainly due to the decrease in the RarcHF. The RarcLF does not suggest any noticeable pattern concerning the mechanical load, except a small increase from 1.7 to 2 MPa, which may be attributed to the increase in the mass transport resistance at this compression range.
As shown in Fig. 5. d) and 5. b), the major reduction in RLF with increasing mechanical compression is due to the decline of the RarcHF (i.e. representative of HF physical processes, including activation phenomena). Up to the time of writing this article, the decrease in the HF physical phenomena / activation resistance with mechanical compression is still not comprehensively addressed in the literature. As a matter of fact, most of the reported studies in this field have focused on mass transport and the ohmic resistances evolution according to mechanical pressure [5-7, 30, 33, 35-36]. A possible explanation for the decrease in RarcHF (leading to a decline in RLF), provided by Dotelli et al. in [31] can be suggested: electron transfer processes, which are responsible of activation losses, are certainly favoured by good contacts between GDL and CL, and increasing mechanical compression helps to reduce contact resistances. Similar interpretation is given by Liu et al. in [34]. However, future investigations still need to be carried out in order to clarify the plausible causes that may lead to the reduction of RarcHF with increasing mechanical compression, and should be the subject of future research [55-57].

5. Conclusion

Our work aims to study the impacts of mechanical compression on the electrical behaviour of a PEMFC. In contrast to previous investigations conducted on cells with restricted active areas [30, 31, 33-35], our experiments involve a relatively large cell, with electrode area measuring 225 cm², thereby enhancing its relevance to potential real-world applications. Initially, analyses were first carried out in [42] using cell voltage monitoring and U-I curves. The earlier findings obtained through steady-state characterisations showed that compression, up to 1.55 MPa, enhances PEMFC performance across all tested conditions (Fig. 1). This result was explained by the prevailing drop in ohmic resistance compared to the increase in

mass transfer losses. In line with [58], it was also shown that mechanical constraints exceeding 1.55 MPa do not lead to any further enhancement in FC voltage.
In this article, EIS is employed as an additional tool to complement the previous steady-state testing methods. The objective is to enhance the deconvolution of the different types of electrical phenomena in the cell under mechanical stress. The investigations are carried out using a gradual increase of mechanical load from 0.35 to 2 MPa, with small increments of 0.15 MPa, which gives a high degree of precision to the study. The EIS analysis is done by studying the evolution, according to mechanical compression, of the ohmic and LF resistances, as well as the LF and HF arc sizes (partly representative of charge transfer and mass transport phenomena). The EIS results confirm what the polarisation curve and cell voltage measurement analyses showed earlier in [42], notably an optimum compression close to 1.55 MPa. The EIS results emphasise the fact that mechanical load reduces mainly the ohmic losses (decrease of the HF resistance from 0.35 to around 1.55 MPa). The significant occurrence of detrimental HF physical phenomena (indicated by the larger size of the HF arc in the EIS spectra) is notable at low compression level (0.35 MPa). However, electron transfer processes are certainly favoured by better contacts between the GDL and the CL, as mechanical compression is increased within the range of 0.35 to 0.80 MPa. This phenomenon is seldom observed and discussed in the existing literature [31, 34]. No significant effect of mechanical stress on mass transport was observed within the studied compression range (0.35 - 2 MPa), except possibly at the highest values (from 1.7 to 2 MPa).
Correlations between in-situ results, reported in this article, and results of additional ex-situ investigations, are also proposed. They mainly show that the evolutions of the ex-situ results (through-plane resistance of the GDL) and the in-situ results (HF resistance) showed a similar reduction tendency with increasing mechanical compression.
In order to understand the impact of mechanical stress on the local phenomena (e.g. current and temperature distributions within the cell), analyses of the PEMFC under mechanical compression were also carried out as a part of this research. The results of this study are suitable for future publications.

Acknowledgments
The authors express their gratitude to the "Région Bourgogne-Franche-Comté" for their support via the ELICOP research project (2015C-4944; 2015-4948) and the co-funding of KHETABI El Mahdi's PhD Thesis (2017 Y_07529). Additionally, the authors extend their appreciation to 3M and Plastic Omnium for their valuable support.

References

[1] Jian Zhao, Xianguo Li. A review of polymer electrolyte membrane fuel cell durability for vehicular applications: Degradation modes and experimental techniques. Energy Conversion and Management 2019;199:112022. https://doi.org/10.1016/j.enconman.2019.112022.

[2] Novalin T, Eriksson B, Proch S, Bexell U, Moffatt C, Westlinder J, Lagergren C, Lindbergh G, Wreland Lindström R. Concepts for preventing metal dissolution from stainless-steel bipolar plates in PEM fuel cells. Energy Conversion and Management 2022;253:115153. https://doi.org/10.1016/j.enconman.2021.115153.

[3] Peng Liang, Diankai Qiu, Linfa Peng, Peiyun Yi, Xinmin Lai, Jun Ni. Contact resistance prediction of proton exchange membrane fuel cell considering fabrication characteristics of metallic bipolar plates. Energy Conversion and Management 2018;169:334-344. https://doi.org/10.1016/j.enconman.2018.05.069.

[4] Mahmoudi AH, Ramiar A, Esmaili Q. Effect of inhomogeneous compression of gas diffusion layer on the performance of PEMFC with interdigitated flow field. Energy Conversion and Management 2016;110:78-89. https://doi.org/10.1016/j.enconman.2015.12.012.

[5] Millichamp J, Mason TJ, Neville TP, Rajalakshmi N, Jervis R, Shearing PR, et al. Mechanisms and effects of mechanical compression and dimensional change in polymer electrolyte fuel cells - A review. Journal of Power Sources 2015;284:305-20. https://doi.org/10.1016/j.jpowsour.2015.02.111.

[6] Dafalla AM, Jiang F. Stresses and their impacts on proton exchange membrane fuel cells: A review. International Journal of Hydrogen Energy 2018;43:2327-48. https://doi.org/10.1016/j.ijhydene.2017.12.033.

[7] Khetabi EM, Bouziane K, Zamel N, François X, Meyer Y, Candusso D. Effects of mechanical compression on the performance of polymer electrolyte fuel cells and analysis through in-situ characterisation techniques - A review. Journal of Power Sources 2019;424:8–26. https://doi.org/10.1016/j.jpowsour.2019.03.071.

[8] Chun JH, Park KT, Jo DH, Kim SG, Kim SH. Numerical modeling and experimental study of the influence of GDL properties on performance in a PEMFC. International Journal of Hydrogen Energy 2011;36:1837-45. https://doi.org/10.1016/j.ijhydene.2010.01.036.

[9] Ismail MS, Damjanovic T, Ingham DB, Pourkashanian M, Westwood A. Effect of polytetrafluoroethylene-treatment and microporous layer-coating on the electrical conductivity of gas diffusion layers used in proton exchange membrane fuel cells. Journal of Power Sources 2010;195:2700-8. https://doi.org/10.1016/j.jpowsour.2009.11.069.

[10] Lim C, Wang CY. Effects of hydrophobic polymer content in GDL on power performance of a PEM fuel cell. Electrochimica Acta 2004;49:4149-56. https://doi.org/10.1016/j.electacta.2004.04.009.

[11] Kong CS, Kim D-Y, Lee H-K, Shul Y-G, Lee T-H. Influence of pore-size distribution of diffusion layer on mass-transport problems of proton exchange membrane fuel cells. Journal of Power Sources 2002;108:185-91. https://doi.org/10.1016/S0378-7753(02)00028-9.

[12] Bultel Y, Wiezell K, Jaouen F, Ozil P, Lindbergh G. Investigation of mass transport in gas diffusion layer at the air cathode of a PEMFC. Electrochimica Acta 2005;51:474-88. https://doi.org/10.1016/j.electacta.2005.05.007.

[13] Park S, Popov BN. Effect of cathode GDL characteristics on mass transport in PEM fuel cells. Fuel 2009;88:2068-73. https://doi.org/10.1016/j.fuel.2009.06.020.

[14] Liu D, Case S. Durability study of proton exchange membrane fuel cells under dynamic testing conditions with cyclic current profile. Journal of Power Sources 2006;162:521-31. https://doi.org/10.1016/j.jpowsour.2006.07.007.

[15] Zhang S, Yuan X, Wang H, Mérida W, Zhu H, Shen J, et al. A review of accelerated stress tests of MEA durability in PEM fuel cells. International Journal of Hydrogen Energy 2009;34:388-404. https://doi.org/10.1016/j.ijhydene.2008.10.012.
[16] Wahdame B, Candusso D, Harel F, François X, Péra M-C, Hissel D, et al. Analysis of a PEMFC durability test under low humidity conditions and stack behaviour modelling using experimental design techniques. Journal of Power Sources 2008;182:429-40. https://doi.org/10.1016/j.jpowsour.2007.12.122.
[17] Lian Y, Zheng W, Yue C, Han S, Ming P. Mass transfer capacity degradation of gas diffusion layer under 1000 hours real-world heavy duty load cycles. International Journal of Heat and Mass Transfer 2024;223:125239. https://doi.org/10.1016/j.ijheatmasstransfer.2024.125239.
[18] Tüber K, Pócza D, Hebling C. Visualization of water buildup in the cathode of a transparent PEM fuel cell. Journal of Power Sources 2003;124:403-14. https://doi.org/10.1016/S0378-7753(03)00797-3.
[19] Satija R, Jacobson DL, Arif M, Werner SA. In situ neutron imaging technique for evaluation of water management systems in operating PEM fuel cells. Journal of Power Sources 2004;129:238-45. https://doi.org/10.1016/j.jpowsour.2003.11.068.
[20] Spernjak D, Prasad AK, Advani SG. Experimental investigation of liquid water formation and transport in a transparent single-serpentine PEM fuel cell. Journal of Power Sources 2007;170:334-44. https://doi.org/10.1016/j.jpowsour.2007.04.020.
[21] Montanini R, Squadrito G, Giacoppo G. Experimental evaluation of the clamping pressure distribution in a PEM fuel cell using matrix-based piezoresistive thin-film. Sensors 2009:6.
[22] Gatto I, Urbani F, Giacoppo G, Barbera O, Passalacqua E. Influence of the bolt torque on PEFC performance with different gasket materials. International Journal of Hydrogen Energy 2011;36:13043-50. https://doi.org/10.1016/j.ijhydene.2011.07.066.
[23] De la Cruz J, Cano U, Romero T. Simulation and in situ measurement of stress distribution in a polymer electrolyte membrane fuel cell stack. Journal of Power Sources 2016;329:273-80. https://doi.org/10.1016/j.jpowsour.2016.08.073.
[24] Wen C-Y, Lin Y-S, Lu C-H. Experimental study of clamping effects on the performances of a single proton exchange membrane fuel cell and a 10-cell stack. Journal of Power Sources 2009;192:475-85. https://doi.org/10.1016/j.jpowsour.2009.03.058.
[25] Alizadeh E, Barzegari M M, Momenifar M, Ghadimi M, Saadat SHM. Investigation of contact pressure distribution over the active area of PEM fuel cell stack. International Journal of Hydrogen Energy 2016;41(4):3062-3071. https://doi.org/10.1016/j.ijhydene33.2015.12.057.
[26] Alizadeh E, Ghadimi M, Barzegari M M, Momenifar M, Saadat S H M. Development of contact pressure distribution of PEM fuel cell's MEA using novel clamping mechanism. Energy 2017;131:92-97. https://doi.org/10.1016/j.energy.2017.05.036
[27] Barzegari M M, Ghadimi M, Momenifar M. Investigation of contact pressure distribution on gas diffusion layer of fuel cell with pneumatic endplate. Applied Energy 2020;263:114663. https://doi.org/10.1016/j.apenergy.2020.114663.
[28] Shi Q, Feng C, Ming P, Tang F, Zhang C. Compressive stress and its impact on the gas diffusion layer: A review. International Journal of Hydrogen Energy 2022;47(6):3994-4009. https://doi.org/10.1016/j.ijhydene.2021.10.058.
[29] Le Carre T, Blachot J-F, Poirot-Crouvezier J-P, Laurencin J. Mechanical response of carbon paper gas diffusion layer under patterned compression. International Journal of Hydrogen Energy 2024;50 Part C:234-247. https://doi.org/10.1016/j.ijhydene.2023.08.104.
[30] Mason TJ, Millichamp J, Shearing PR, Brett DJL. A study of the effect of compression on the performance of polymer electrolyte fuel cells using electrochemical

impedance spectroscopy and dimensional change analysis. International Journal of Hydrogen Energy 2013;38:7414-22. https://doi.org/10.1016/j.ijhydene.2013.04.021.
[31] Dotelli G, Omati L, Gallo Stampino P, Grassini P, Brivio D. Investigation of gas diffusion layer compression by electrochemical impedance spectroscopy on running polymer electrolyte membrane fuel cells. Journal of Power Sources 2011;196:8955-66. https://doi.org/10.1016/j.jpowsour.2011.01.078.
[32] Mason TJ, Millichamp J, Neville TP, Shearing PR, Simons S, Brett DJL. A study of the effect of water management and electrode flooding on the dimensional change of polymer electrolyte fuel cells. Journal of Power Sources 2013;242:70-7. https://doi.org/10.1016/j.jpowsour.2013.05.045.
[33] Zhao C, Xing S, Liu W, Chen M, Wang Y, Wang H. An experimental study on pressure distribution and performance of end-plate with different optimization parameters for air-cooled open-cathode LT-PEMFC. International Journal of Hydrogen Energy 2020;45(35):17902-17915. https://doi.org/10.1016/j.ijhydene.2020.04.270.
[34] Liu J, Tan J, Yang W, Li Y, Wang C. Better electrochemical performance of PEMFC under a novel pneumatic clamping mechanism. Energy 2021;229:120796. https://doi.org/10.1016/j.energy.2021.120796.
[35] Sim J, Kang M, Min K. Effects of ratio variation in substrate and micro porous layer penetration on polymer exchange membrane fuel cell performance. International Journal of Hydrogen Energy 2021;46(35):18615-18629. https://doi.org/10.1016/j.ijhydene.2021.03.029.
[36] Sunil K. Sethy, Amit C. Bhosale. A unique clamping mechanism for a cylindrical PEMFC for an enhanced performance. Journal of Power Sources 2024;600:234258. https://doi.org/10.1016/j.jpowsour.2024.234258.
[37] El Oualid S, Lachat R, Candusso D, Meyer Y. Characterization process to measure the electrical contact resistance of Gas Diffusion Layers under mechanical static compressive loads. International Journal of Hydrogen Energy 2017;42:23920-31. https://doi.org/10.1016/j.ijhydene.2017.03.130.
[38] Khetabi EM. Behavioural analysis of PEM fuel cell components and research of causal relationships between in-situ and ex-situ observed performances. PhD Thesis of Université Paris-Saclay, 2021.
[39] Bouziane K. Study of the relationship between the performance of PEM fuel cell components and their behaviours in stacks operated in the complete system. Development of electrical and mechanical characterization techniques. PhD Thesis of Université Paris-Saclay, 2021.
[40] Bouziane K, Khetabi EM, Lachat R, Zamel N, Meyer Y, Candusso D. Impact of cyclic mechanical compression on the electrical contact resistance between the gas diffusion layer and the bipolar plate of a polymer electrolyte membrane fuel cell. Renewable Energy 2020;153:349-61. https://doi.org/10.1016/j.renene.2020.02.033.
[41] Charbonné C, Dhuitte ML, Bouziane K, Chamoret D, Candusso D, Meyer Y. Design of experiments on the effects of linear and hyperelastic constitutive models and geometric parameters on polymer electrolyte fuel cell mechanical and electrical behaviour. International Journal of Hydrogen Energy 2021;46(26):13775-13790. https://doi.org/10.1016/j.ijhydene.2021.02.122
[42] Khetabi EM, Bouziane K, François X, Lachat R, Meyer Y, Candusso D. In-situ experimental investigations to study the impact of mechanical compression on the PEMFC - Analysis of the global cell performance. International Journal of Hydrogen Energy 2024;56:1257-1272. https://doi.org/10.1016/j.ijhydene.2023.12.293.
[43] Fuel Cell and Battery Test Equipment | Greenlight Innovation. https://www.greenlightinnovation.com/.
[44] Material Mates Italia Srl. Material Mates Italia Srl. https://www.mmates.it/.

[45] balticFuelCells GmbH: Innovation in fuel cell technologies. https://www.balticfuelcells.de/defaultE.html.
[46] NafionTM XL. https://www.fuelcellstore.com/nafion-xl.
[47] Robert M, El Kaddouri A, Perrin J-C, Mozet K, Daoudi M, Dillet J, et al. Effects of conjoint mechanical and chemical stress on perfluorosulfonic-acid membranes for fuel cells. Journal of Power Sources 2020;476:228662. https://doi.org/10.1016/j.jpowsour.2020.228662.
[48] Fuel Cells on the Rise. SGL Carbon. https://www.sglcarbon.com/en/for-a-smarter-world/fuel-cells-on-the-rise/.
[49] (PDF) SIGRACET® Gas Diffusion Layers for PEM Fuel Cells, Electrolyzers and Batteries (White Paper). https://www.researchgate.net/publication/295859224_SIGRACETR_Gas_Diffusion_Layers_for_PEM_Fuel_Cells_Electrolyzers_and_Batteries_White_Paper.
[50] Bi-polar Plates. https://www.schunk-carbontechnology.com/en/products/produkte-detail/bipolar-plates.
[51] Pérez-Page M, Pérez-Herranz V. Study of the electrochemical behaviour of a 300 W PEM fuel cell stack by Electrochemical Impedance Spectroscopy. International Journal of Hydrogen Energy 2014;39:4009-15. https://doi.org/10.1016/j.ijhydene.2013.05.121.
[52] Tang Z, Huang Q-A, Wang Y-J, Zhang F, Li W, Li A, et al. Recent progress in the use of electrochemical impedance spectroscopy for the measurement, monitoring, diagnosis and optimization of proton exchange membrane fuel cell performance. Journal of Power Sources 2020;468:228361. https://doi.org/10.1016/j.jpowsour.2020.228361.
[53] Pivac I, Barbir F. Inductive phenomena at low frequencies in impedance spectra of proton exchange membrane fuel cells - A review. Journal of Power Sources 2016;326:112-9. https://doi.org/10.1016/j.jpowsour.2016.06.119.
[54] Nitta I, Hottinen T, Himanen O, Mikkola M. Inhomogeneous compression of PEMFC gas diffusion layer: Part I. Experimental. Journal of Power Sources 2007;171:26-36. https://doi.org/10.1016/j.jpowsour.2006.11.018.
[55] Zhang J, Song C, Zhang J, Baker R, Zhang L. Understanding the effects of backpressure on PEM fuel cell reactions and performance. Journal of Electroanalytical Chemistry 2013;688:130-6. https://doi.org/10.1016/j.jelechem.2012.09.033.
[56] Iftikhar MU, Riu D, Druart F, Rosini S, Bultel Y, Retière N. Dynamic modeling of proton exchange membrane fuel cell using non-integer derivatives. Journal of Power Sources 2006;160:1170-82. https://doi.org/10.1016/j.jpowsour.2006.03.044.
[57] Kongkanand A, Gu W, Mathias MF. Proton-Exchange Membrane Fuel Cells with Low-Pt Content. In: Meyers RA, editor. Encyclopedia of Sustainability Science and Technology, New York, NY: Springer; 2017, p. 1-20. https://doi.org/10.1007/978-1-4939-2493-6_1022-1.
[58] Ahmad M, Harrison R, Meredith J, Bindel A, Todd B. Validation of a fuel cell compression spring equivalent model using polarisation data. International Journal of Hydrogen Energy 2017;42:8109-8118. http://dx.doi.org/10.1016/j.ijhydene.2017.01.216.